Applied Catalysis B: Environmental 218 (2017) 409–419

Contents lists available at ScienceDirect

Applied Catalysis B: Environmental

journal homepage: www.elsevier.com/locate/apcatb

Deactivation of Pt/SiO_2-ZrO_2 diesel oxidation catalysts by sulphur, phosphorus and their combinations

Ari Väliheikki[a,d], Marja Kärkkäinen[a], Mari Honkanen[b], Olli Heikkinen[c], Tanja Kolli[a], Kauko Kallinen[d], Mika Huuhtanen[a], Minnamari Vippola[b], Jouko Lahtinen[c], Riitta L. Keiski[a,*]

[a] Environmental and Chemical Engineering, Faculty of Technology, University of Oulu, POB 4300, FI-90014 University of Oulu, Finland
[b] Department of Materials Science, Tampere University of Technology, POB 589, FI-33101 Tampere, Finland
[c] Department of Applied Physics, Aalto University, POB 15100, FI-00076 Aalto, Finland
[d] Dinex Ecocat Oy, POB 20, Vihtavuorentie 162, FI-41331 Vihtavuori, Finland

ARTICLE INFO

Article history:
Received 15 March 2017
Received in revised form 19 June 2017
Accepted 22 June 2017
Available online 24 June 2017

Keywords:
DOC
Sulphur dioxide
Phosphorus
Platinum
Silicon-zirconium oxide

ABSTRACT

The impact of sulphur, phosphorus and water and their co-exposure on a monolith-type Pt/SiO_2-ZrO_2 diesel oxidation catalyst was investigated. The accelerated laboratory-scale sulphur treatments for Pt/SiO_2-ZrO_2 were done with and without water (S- and SW-treatments, respectively) at 400 °C. Similarly, the phosphorus treatment with water (PW-treatment) as well as the co-exposure of phosphorus, sulphur and water (PSW-treatment) were also done to find out the interactions between the impurities. The studied catalysts were characterized by using several techniques and the activity of the catalyst was tested in lean diesel exhaust gas conditions. Based on the XPS and the elemental analysis, more phosphorus was adsorbed on the Pt/SiO_2-ZrO_2 catalyst than sulphur. Sulphur, in the presence and absence of water, was found to have a negligible effect on the CO and C_3H_6 light-off temperatures (T_{90}) over the fresh Pt/SiO_2-ZrO_2, whereas the T_{90} values of CO and C_3H_6 increased by 30–45 °C as a result of the PW-treatment and by 15–35 °C after the PSW-treatment. Based on the Transmission electron microscope (TEM) analyses, no morphological changes on the Pt/SiO_2-ZrO_2 surfaces were observed due to the phosphorus treatment. Therefore, the reason for the lower activity after the PW-treatment could be the formation of phosphates that are decreasing the specific surface area of the catalyst, blocking the accessibility of the reactants to the catalyst pores and active sites. However, it is worth noting that sulphur decreased the amount of adsorbed phosphorus and thus, inhibited the poisoning effect of phosphorus.

1. Introduction

The diesel oxidation catalyst (DOC) is one of the most important parts of diesel exhaust gas after-treatment systems along with the diesel particulate filter (DPF) and the selective catalytic reduction (SCR) unit. The role of DOC is to oxidize harmful emissions such as carbon monoxide (CO), unburned hydrocarbons (UHCs) and soluble organic fraction (SOF) of particulates. In addition, the DOC has the ability to oxidize nitrogen monoxide (NO) to nitrogen dioxide (NO_2) which improves the removal efficiency of NO_x in the following SCR unit. The European Union (EU) has set strict regulations towards the emissions from mobile sources, including light-duty vehicles [1]. To fulfil the EU emission standards, the high performance of the emission purification units are required in the exhaust gas treatment systems are needed. To achieve high activity over a long-term period, the DOC needs to be resistant towards chemical impurities e.g. sulphur and phosphorus present in the exhaust gas stream. Sulphur is generally present in the form of sulphur dioxide (SO_2) in the exhaust of coal and petroleum derivatives (gasoline, diesel) combustion, and fuel used in shipping [2,3]. Phosphorus compounds can be originated e.g. from biofuels and lubricant oils used [4,5]. Both sulphur and phosphorus have been widely reported to decrease the activity of platinum on aluminium oxide (Pt/Al_2O_3) catalysts [6–10] which are the most used and the most efficient materials in DOCs [4,7,8,11]. Thus, there is a need for novel diesel oxidation

Abbreviations: SW, sulphur + water; PW, phosphorus + water; PSW, phosphorus + sulphur + water.

* Corresponding author.
E-mail addresses: avh@dinex.fi (A. Väliheikki), marja.karkkainen@oulu.fi (M. Kärkkäinen), mari.honkanen@tut.fi (M. Honkanen), olli.heikkinen@aalto.fi (O. Heikkinen), tanja.kolli@welho.com (T. Kolli), kki@dinex.fi (K. Kallinen), mika.huuhtanen@oulu.fi (M. Huuhtanen), minnamari.vippola@tut.fi (M. Vippola), jouko.lahtinen@aalto.fi (J. Lahtinen), riitta.keiski@oulu.fi (R.L. Keiski).

http://dx.doi.org/10.1016/j.apcatb.2017.06.068
0926-3373/

catalysts especially for marine and stationary applications that use biofuels and lubricant oils, which may contain impurities such as phosphorus and sulphur.

One option to substitute the commonly used Pt/Al_2O_3 catalysts is the Pt/SiO_2-ZrO_2 catalyst which has also shown high activity e.g. in CO oxidation [12]. Silicon dioxide (SiO_2) was found to have well controlled and known properties e.g. small particle size, high specific surface area and high porosity as a support material [13,14]. In addition, SiO_2 is reported to be inert to sulphur poisoning [15–17] which is due to the lack of basicity of the material [12]. The addition of zirconium dioxide (ZrO_2) on a SiO_2 support is reported to increase the Pt dispersion and hydrothermal stability of the catalyst [9,12]. Furthermore, the Pt/SiO_2-ZrO_2 catalysts are reported to have a higher activity in CO oxidation than the Pt/SiO_2 based catalysts [12]. These attractive features make the Pt/SiO_2-ZrO_2 catalyst a promising material for DOC applications. The effect of sulphur on the Pt/SiO_2-ZrO_2 catalyst has been investigated in a few studies [9,12]. According to Kim et al. [12], sulphur increases the CO light-off temperature over the Pt/SiO_2-ZrO_2 catalyst by ~40 °C, but still the Pt/SiO_2-ZrO_2 catalyst was found to be more resistant towards SO_2 compared to the Pt/Al_2O_3 and Pt/SiO_2 catalysts. In Park et al. [9], it has been presented that sulphur decreases slightly the activity of the Pt/SiO_2-ZrO_2 catalyst in the NO reduction. Based on our best knowledge, the effect of phosphorus on the SiO_2-ZrO_2 based catalysts has not yet been investigated earlier. Thus, the impact of both sulphur and phosphorus and their co-effect on the Pt/SiO_2-ZrO_2 catalysts are studied and reported in this study.

The aim of this work was to find out the effects of sulphur, phosphorus and water and their co-exposure on the Pt/SiO_2-ZrO_2 catalyst morphology and its performance. The treatment with gaseous SO_2 for the Pt/SiO_2-ZrO_2 catalyst was done at 400 °C in the absence and presence of water (denoted as S- and SW-treatments, respectively). The water and phosphorus treatments (W- and PW-treatments, respectively) as well as the co-exposure of phosphorus and sulphur (PSW-treatment) were also studied at the same conditions. Several characterization techniques such as XPS, DRIFTS, FESEM, TEM, XRD, BET/BJH and NO-TPD have been used to identify the morphological and chemical changes on the catalyst surface caused by the treatments. The activity of fresh, S-, W-, SW-, PW-, and PSW-treated catalysts was studied using a model diesel exhaust gas flow ($CO + C_3H_6 + NO + H_2O + O_2 + N_2$).

2. Experimental

2.1. Studied materials

The studied materials were two metallic monoliths provided by Dinex Ecocat Oy. The materials contained 0 or 0.5 wt-% of platinum as the active material on the silicon-zirconium oxide support (marked as SiO_2-ZrO_2 and Pt/SiO_2-ZrO_2, respectively). The support material was silicon-zirconium mixed oxide (80 wt-%) with SiO_2 as a binder (20 wt-%) that resulted in the SiO_2/ZrO_2 weight ratio of 30/70 in the final coating.

2.2. Treatments

The monolith-type samples containing the SiO_2-ZrO_2 support or the Pt/SiO_2-ZrO_2 catalyst were placed in a vertically positioned tubular quartz reactor. The diameter of the sample was 10 mm and length 37 mm. The total flow was kept constant (1 dm^3/min) and the gas hourly space velocity (GHSV) was 21,000 h^{-1}. The reactor was heated to 400 °C (with the heating rate of 10 °C/min) under a gas mixture of 2 vol-% of O_2, and balance N_2. Then, the laboratory-scale accelerated treatments using water (H_2O), sulphur dioxide (SO_2) or aqueous ammonium phosphate ($(NH_4)_2HPO_4$) for 5 h at 400 °C and the mixtures of these were carried out. These treatments were done in the gas phase according to the following compositions:

1. S-treatment: 100 ppm SO_2, 10% air, and balance N_2
2. W-treatment: 10% H_2O, 10% air, and balance N_2
3. SW-treatment: 100 ppm SO_2, 10% H_2O, 10% air, and balance N_2
4. PW-treatment: aqueous solution of phosphorus containing 10% H_2O with $c((NH_4)_2HPO_4) = 0.13$ M, 10% air, and balance N_2
5. PSW-treatment: aqueous solution of phosphorus containing 10% H_2O with $c((NH_4)_2HPO_4) = 0.13$ M, 100 ppm SO_2, 10% air, and balance N_2

2.3. Characterizations

X-ray photoelectron spectroscopy (XPS) was used for characterizing the chemical states and concentrations of different elements on the catalyst and support. The spectrometer (Surface Science Laboratories SSX-100) was equipped with a monochromatic Al K_α X-ray beam and had a base pressure of 5×10^{-10} mbar. The samples were pressed as a powder form on the indium films prior to placing them into the measurement chamber. In order to prevent charging of the samples during measurements, an electron flood gun was used. The Shirley background subtraction was employed before fitting the Gauss-Lorentz functions to the experimental data. The binding energy values in the acquired spectra were calibrated by setting carbon 1s line at 284.6 eV. Carbon and indium were excluded from the compositional analysis.

The nature of compounds adsorbed on the catalyst surface were analysed using the Diffuse Reflectance Infrared Fourier Transform Spectroscopy (DRIFTS). The experiments were carried out using the Bruker Vertex V80 vacuum FTIR spectrometer with a Harrick Praying Mantis™ DRIFT unit and an environmental cell. The sample was measured at 25 °C in atmospheric pressure using a mirror as a reference. The DRIFT spectra were recorded in the range of 4000–400 cm^{-1} with a resolution of 4 cm^{-1} with 32 spectra in each measurement.

The structure of the fresh and treated catalysts and supports was studied by a field emission scanning electron microscope (FESEM, Zeiss ULTRAplus) equipped with an energy dispersive X-ray spectrometer (EDS, INCA Energy 350 with INCAx-act silicon drift detector, Oxford Instruments). In addition, a transmission electron microscope (TEM, Jeol JEM-2020) equipped with an EDS (Noran Vantage with Si(Li) detector, Thermo Scientific) was used. The cross-sectional samples for FESEM studies were prepared with a conventional metallographic sample preparation technique including moulding of the monolith in resin, grinding and polishing and finally carbon coating to avoid sample charging. In the TEM studies, powdered samples or cross-sectional samples were used. The powdered TEM samples were mixed with ethanol and dispersed onto a copper grid with a holey carbon film. The cross-sectional TEM samples were prepared by placing the two small pieces of the monolith on a titanium grid by carbon glue and followed by thinning the grid with a dimple grinder (Model 656, Gatan Inc.) and a precision ion polishing system (PIPS, Model 691, Gatan Inc.).

The structure of scraped catalyst powders was also studied using an X-ray diffractometer (XRD, Empyrean, PANanlytical with the PIXcel^{3D} detector using Cu Kα radiation). Crystallite sizes were determined from the XRD patterns with the aid of the HighScore plus software based on the Scherrer equation and phases were identified by using the database (PDF-4+ 2014) from International Centre for Diffraction Data (ICDD).

The determination of specific surface areas (S_{BET}), pore sizes and pore volumes of the fresh, S-, W-, SW-, PW-, and PSW-treated Pt/SiO_2-ZrO_2 catalysts were done by N_2 adsorption at −196 °C

Table 1
Binding energies (eV) measured with XPS over the SiO_2-ZrO_2 support and Pt-loaded catalyst on fresh and after the treatments.

		Pt $4d_{5/2}$	P 2s	S 2p	O 1s		Si 2s	Zr $3d_{5/2}$
Support								
Fresh					532.5	530.2	154.0	182.3
W	inlet				532.1	529.8	153.6	182.0
	outlet				532.5	530.2	154.0	182.3
S	inlet			–	532.3	530.0	153.6	182.3
	outlet			168.7	531.9	529.6	153.7	181.9
SW	inlet			168.8	532.0	529.7	153.8	182.3
	outlet			169.8	532.4	530.1	153.6	182.7
PW	inlet		190.1		532.4	530.1	154.4	182.5
	outlet		190.5		531.5	529.2	153.0	181.7
PSW	inlet		190.3	–	531.8	529.5	153.7	182.0
	outlet		190.2	170.8	532.3	530.0	153.6	181.9
Catalyst								
Fresh		313.1			532.0	529.7	153.4	182.0
W	inlet	313.9			532.2	529.9	153.7	181.9
	outlet	314.8			532.6	530.3	154.3	181.8
S	inlet	313.6		169.2	532.3	530.0	153.8	182.7
	outlet	314.5		169.1	532.5	530.2	153.8	182.7
SW	inlet	314.1		169.4	533.4	531.1	154.6	183.1
	outlet	314.3		169.8	532.6	530.3	153.8	182.6
PW	inlet	314.1	190.4		531.0	528.7	153.1	182.3
	outlet	313.2	190.9		531.3	529.0	153.6	182.2
PSW	inlet	313.6	190.4	–	531.6	529.3	153.6	182.1
	outlet	313.9	190.7	168.8	532.2	529.9	153.8	182.1

using a Micrometrics ASAP2020 analyzer. The specific surface areas (m^2/g) were determined according to the Brunauer-Emmett-Teller (BET) theory. The pore volumes (cm^3/g) and the pore sizes (nm) were found out based on the Barrett-Joyner-Halenda (BJH) theory.

The NO adsorption on the fresh, S-, W-, SW-, PW-, and PSW-treated Pt/SiO_2-ZrO_2 catalysts was tested in temperature programmed experiments. The catalyst was pre-treated for 15 min at 300 °C in a N_2 flow followed by cooling to 25 °C in a N_2 flow. Thereafter, NO adsorption (1% NO/N_2, 30 cm^3/min) was done for 30 min at 25 °C. The reactor was purged with N_2 for 15 min. NO desorption was studied under a N_2 flow (1 dm^3/min) at 25–500 °C with a heating rate of 20 °C/min. The concentrations of compounds (NO, NO_2 and N_2O) were analysed using a Gasmet™ FT-IR gas analyser.

2.4. Activity tests

The laboratory-scale activity tests were done for the fresh, S-, W-, SW-, PW-, and PSW-treated Pt/SiO_2-ZrO_2 catalyst. The catalyst monolith was packed in a quartz tube reactor. The catalyst activity was studied in lean diesel exhaust gas conditions with the following gas mixture: 500 ppm CO, 300 ppm C_3H_6, 1000 ppm NO, 10 vol-% H_2O, 12 vol-% O_2 and balance N_2. The total flow was kept constant (1 dm^3/min) and GHSV was 34,000 h^{-1}. The concentrations of the gaseous compounds (CO, C_3H_6, CH_4, CO_2, NO, NO_2, N_2O and H_2O) were analysed by a Gasmet™ FT-IR gas analyser. The volume of O_2 was analysed by using a paramagnetic oxygen analyser (ABB Advanced Optima). The temperature of the catalyst was increased

Table 2
Elemental compositions (in wt-%) on the SiO_2-ZrO_2 support and the Pt/SiO_2-ZrO_2 catalyst surface after the treatments (analysed by XPS).

		Pt	P	S	O	Si	Zr
Support							
Fresh					47	22	31
W	inlet				46	22	33
	outlet				46	21	33
S	inlet			0.0	45	21	34
	outlet			0.2	49	24	27
SW	inlet			0.2	47	22	31
	outlet			0.2	45	21	33
PW	inlet		0.2		47	23	30
	outlet		0.1		50	22	28
PSW	inlet		1.9	0.0	50	21	27
	outlet		0.4	0.2	48	22	30
Catalyst							
Fresh		0.4			44	21	34
W	inlet	0.5			48	23	28
	outlet	0.5			47	22	31
S	inlet	0.6		0.4	46	22	31
	outlet	0.7		0.4	47	20	32
SW	inlet	0.6		0.5	48	22	28
	outlet	0.5		0.9	48	19	31
PW	inlet	0.4	7.9		49	15	28
	outlet	0.5	6.6		50	18	25
PSW	inlet	0.7	4.0	0.0	50	19	26
	outlet	0.5	1.9	0.1	51	19	28

Table 3
Crystallite sizes of the fresh, SW-, PW-, and PSW-treated Pt/SiO_2-ZrO_2 catalysts and SiO_2-ZrO_2 support (determined from XRD patterns).

	Pt/SiO_2-ZrO_2 catalyst				SiO_2-ZrO_2 support			
	Fresh	SW	PW	PSW	Fresh	SW	PW	PSW
Pt[a]	14	16	18	16	–	–	–	–
ZrO_2[b]	6 nm	6 nm	7 nm	6 nm	6 nm	6 nm	6 nm	6 nm

[a] Determined from Pt-peak at $2\theta = 39.7^\circ$ with the Scherrer equation (shape factor 0.9).
[b] Determined from ZrO_2-peak at $2\theta = 30.5^\circ$ with the Scherrer equation (shape factor 0.9).

from 25 °C to 300 °C (the heating rate of 5 °C/min) in the reaction gas flow. The water was fed at 125 °C by a peristaltic pump. The catalyst was kept at 300 °C in steady state conditions for 15 min followed by cooling down to room temperature under the reaction gas mixture. This procedure was repeated twice. The conversions of CO, C_3H_6 and NO were calculated based on data gained during the second ramp.

3. Results and discussion

3.1. Fresh and water treated catalyst

The chemical states and adsorbed surface compounds of the fresh Pt/SiO_2-ZrO_2 catalyst and the SiO_2-ZrO_2 support were studied using XPS and DRIFT. The binding energy values for the most prominent photoelectron lines of each surface element determined by XPS are shown in Table 1. The observed Pt $4d_{5/2}$ line indicates that platinum is in the metallic form (Pt) in the fresh catalyst [18]. The binding energies of Si 2s and Zr $3d_{5/2}$ can be attributed to SiO_2 and ZrO_2, respectively. Two overlapping O 1s lines were detected and their relative intensities were in accordance with the atomic concentration ratios between silicon and zirconium (Table 2). Thus, these two lines were attributed to oxygen in SiO_2 and ZrO_2, which corresponds to their measured binding energy values. According to the DRIFT results, the spectra of the SiO_2-ZrO_2 support and Pt/SiO_2-ZrO_2 catalyst were almost identical (Fig. 1). The small peak observed around 1630 cm^{-1} can be attributed to molecular H_2O bending. [19–21]. In the range of 1140–1300 cm^{-1} the broad band can be attributed to asymmetric stretching vibrations of the Si—O—Si band [19,22]. The small peak at 1092 cm^{-1} corresponds to the vibration of the Si—O—Si band [14,21,23]. The peaks at 980 cm^{-1} and 818 cm^{-1} correspond to the Si—OH stretching and the symmetric Si—O—Si stretching, respectively [19,24]. The bands at 736 cm^{-1} can be attributed to the Zr—O band [25,26].

The structures of the fresh Pt/SiO_2-ZrO_2 catalyst and SiO_2-ZrO_2 support were studied by FESEM, TEM and XRD. According to the FESEM results (Fig. 2a), the Pt/SiO_2-ZrO_2 catalyst has a layered structure and based on the EDS line analyses, the amount of silicon increases and zirconium decreases towards the metallic monolith. Pt particles are too small to be detected with FESEM. Based on the TEM results (Fig. 2b), the support material has zirconium oxide and silicon oxide based areas. The selected area electron diffraction (SAED) patterns of the zirconium oxide based areas have crystalline rings indicating the nanocrystalline ZrO_2. In addition, the ZrO_2 based areas contain small (~10 nm) Pt particles. The SAED patterns from the SiO_2 based areas have diffuse rings indicating mainly an amorphous structure. The XRD patterns of the fresh Pt/SiO_2-ZrO_2 catalyst and SiO_2-ZrO_2 support are presented in Fig. 3 and the average crystallite sizes of Pt and ZrO_2 are presented in Table 3. Based on the XRD results, Pt in the catalyst is in a metallic form with the average crystallite size of 14 nm agreeing well with the XPS and TEM results. Furthermore, ZrO_2 with the average crystallite size of 6 nm was detected from the XRD results (Fig. 3, Table 3), which is in agreement with the TEM and XPS results. Contrary to the TEM results, amorphous SiO_2 was not detected by XRD probably due to its amorphous nanopowder characteristics and because the crystalline ZrO_2 dominates in the XRD pattern (Fig. 3).

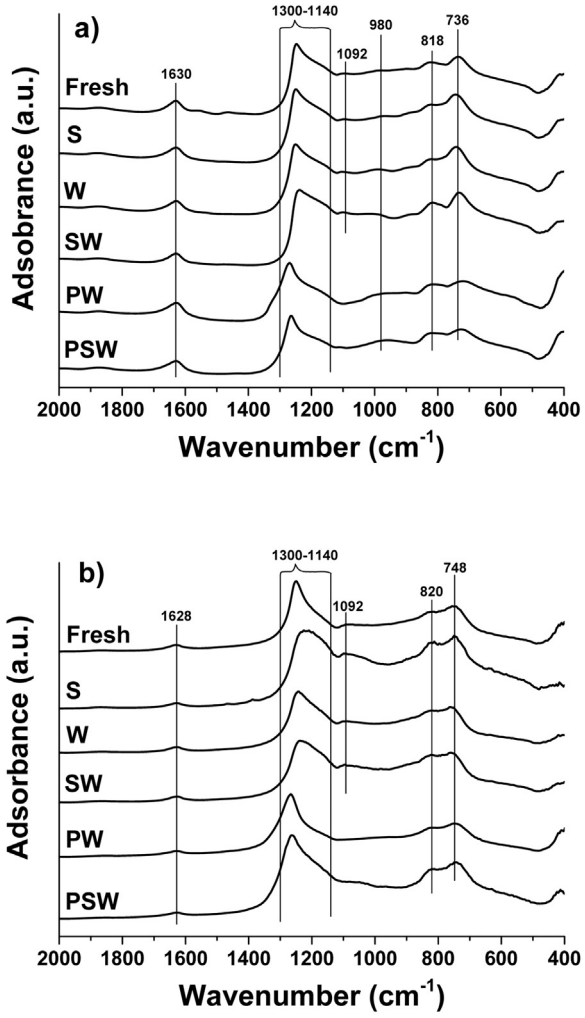

Fig. 1. Infrared spectra of fresh, S-, W-, SW-, PW-, and PSW-treated Pt/SiO_2-ZrO_2 catalysts (a) and SiO_2-ZrO_2 support (b) in the region of 2000–400 cm^{-1}.

The conversions of CO, C_3H_6 and NO as well as the formation of NO_2 and N_2O over the fresh Pt/SiO_2-ZrO_2 catalyst are shown in Fig. 4. The light-off temperatures of 50% and 90% for both CO and C_3H_6 as well as the maximum NO conversions are summarized in Table 4. The CO conversion is around 15% at 125 °C and reached the 100% conversion at 205 °C. The C_3H_6 oxidation reaction starts at temperatures around 160 °C and 100% conversion was achieved at 230 °C. The formation of NO_2 started at 210 °C at the same temperature where the CO oxidation reaction is completed. The NO oxidation to NO_2 is a desired reaction because the ratio of $NO:NO_2 \approx 1$ improves the performance of the down-stream exhaust gas purification units (the SCR converter and particulate filter) [27–29]. During the activity test, the N_2O formation was also observed being below 40 ppm at 180–300 °C. The N_2O formation

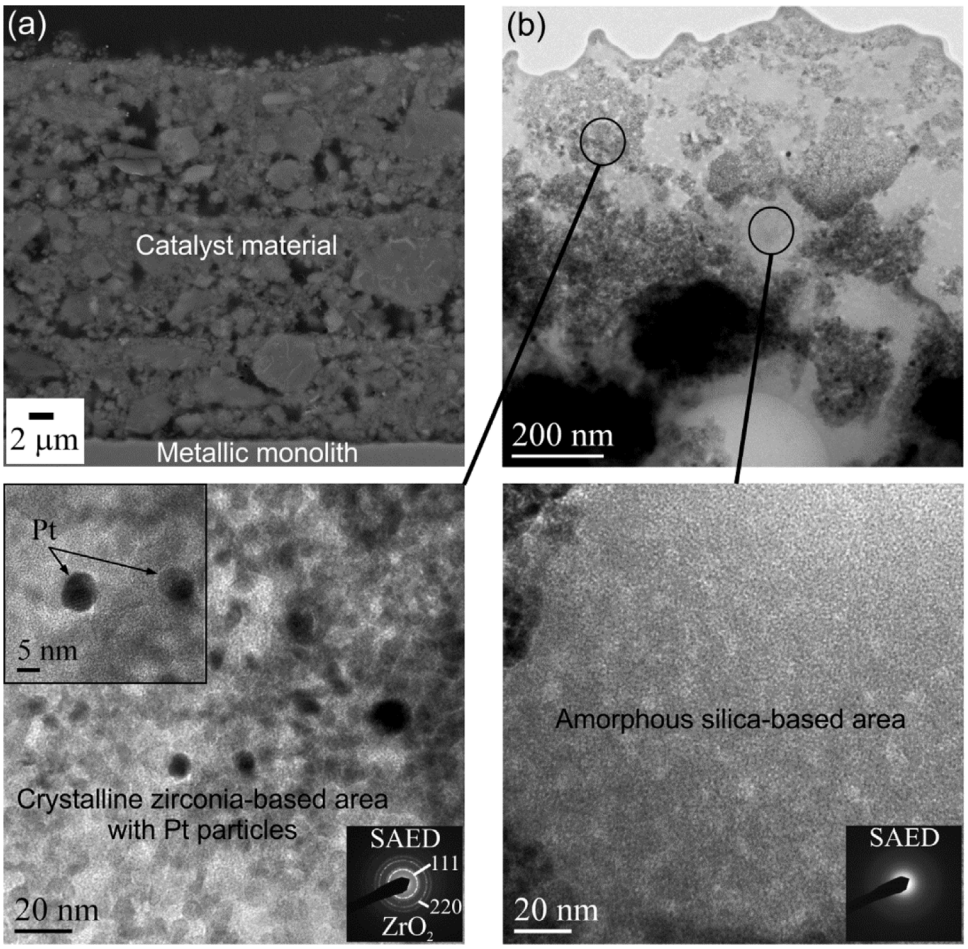

Fig. 2. The cross-sectional FESEM image (a) and the cross-sectional TEM images of the fresh Pt/SiO_2-ZrO_2 catalyst (b) with higher magnification images with SAED patterns from the corresponding areas.

could be due to the overall reaction (1) according to the study done by Khosravi et al. [30]:

$$C_3H_6 + 2NO + 4O_2 \rightarrow N_2O + 3H_2O + 3CO_2 \quad (1)$$

In our earlier study [31], CO, C_3H_6 and NO oxidation activity on Pt/Al_2O_3 and $PtPd/Al_2O_3$ catalysts have been studied. Comparison between the fresh Pt/Al_2O_3, $PtPd/Al_2O_3$ and Pt/Al_2O_3 shows that the light-off temperature over the fresh Pt/SiO_2-ZrO_2 catalyst in C_3H_6 oxidation is moderately lower (~30 °C) than that over the fresh Pt/Al_2O_3 catalyst, but only slightly lower (~10 °C) than over the fresh $PtPd/Al_2O_3$ catalyst in the entire temperature range stud-

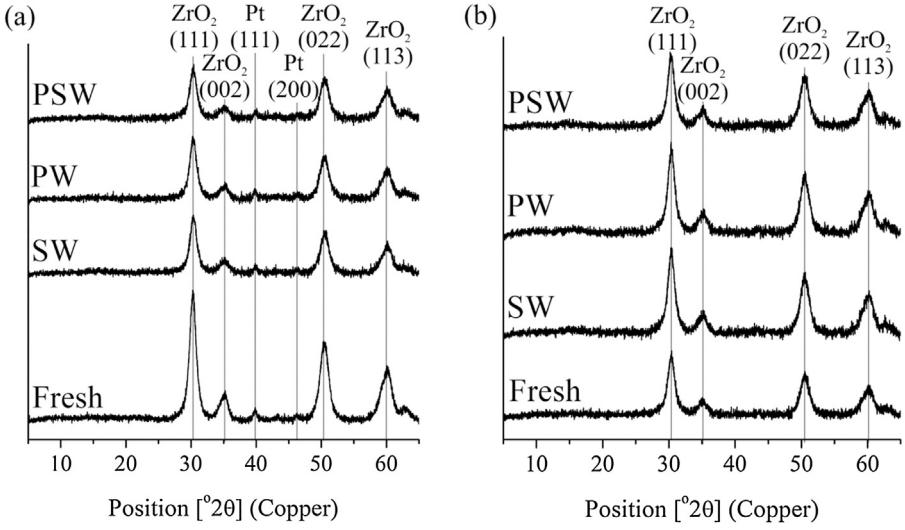

Fig. 3. XRD patterns of the fresh, SW-, PW-, and PSW-treated Pt/SiO_2-ZrO_2 catalysts (a) and SiO_2-ZrO_2 support (b).

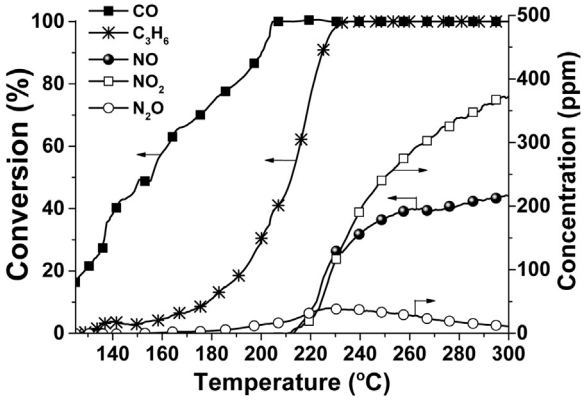

Fig. 4. CO, C_3H_6 and NO conversions (black symbols) as well as NO_2 and N_2O formation (white symbols) over the fresh Pt/SiO_2-ZrO_2 catalyst as a function of temperature. Reaction gas mixture: 500 ppm CO, 300 ppm C_3H_6, 1000 ppm NO, 10 vol-% H_2O, 12 vol-% O_2 and balance N_2. Heating rate: 5 °C/min, Total flow: 1000 ml/min, GHSV: 34,000 h^{-1}.

Table 4
Light-off temperatures (T_{50} and T_{90}) for CO and C_3H_6 oxidation and maximum NO conversion over fresh and treated Pt/SiO_2-ZrO_2 catalysts. Reaction gas mixture: 500 ppm CO, 300 ppm C_3H_6, 1000 ppm NO, 10 vol-% H_2O, 12 vol-% O_2 and balance N_2. Heating rate: 5 °C/min, Total flow: 1000 ml/min, GHSV: 34,000 h^{-1}.

Catalyst	T_{50} (°C)		T_{90} (°C)		Max conversion (%)
	CO	C_3H_6	CO	C_3H_6	NO
Fresh	156	212	200	225	44
S	158	205	195	226	45
W	160	208	204	246	36
SW	161	207	195	227	39
PW	192	234	230	270	17
PSW	167	220	215	261	21

ied. Instead, the NO oxidation activity is in the same level between the fresh Pt/Al_2O_3 and Pt/SiO_2-ZrO_2 catalysts.

The NO-TPD experiments are done to obtain information about the adsorption-desorption behaviour of NO (Figs. 5 and 6). Three NO desorption peaks on the fresh Pt/SiO_2-ZrO_2 were observed at 70, 150 and 280 °C. The NO-TPD results indicate that NO is adsorbed on the catalyst surface and therefore the formation of NO_2 and N_2O is possible. In addition, the NO conversions in activity tests were negligible at temperatures below 200 °C. Alternatively, NO and NO_2 were found to be desorbed from the catalyst and the parent support above 25 °C in the NO-TPD in the case of no competitive reactants (i.e. CO or C_3H_6) were present (Figs. 5 and 6).

Water treatment has found to decrease slightly the activity of the CeZr oxide and the Al_2O_3 based catalyst [31–33]. Thus, the effect of water treatment on the Pt/SiO_2-ZrO_2 catalyst was investigated. The water treatment had a negligible effect on the CO and C_3H_6 oxidations at temperatures below 200 °C. At temperatures above 220 °C, the W-treatment increased the C_3H_6 light-off temperature (T_{90}) by around 20 °C. Similarly, the W-treatment decreased the NO conversion by 5–10 percentage points in the temperature range of 230–300 °C. The reason for the decreased activity could be due to the competing adsorption of H_2O [34], which diminishes the number of active sites available for oxidation reactions. According to the NO-TPD results, the W-treatment decreased the amount of desorbed NO and NO_2 (Table 5). The W-treatment also decreased both the BET surface areas and BJH pore volumes slightly (Table 6). However, the XPS and DRIFT results did not reveal any significant changes on the studied catalyst surfaces after the water treatment.

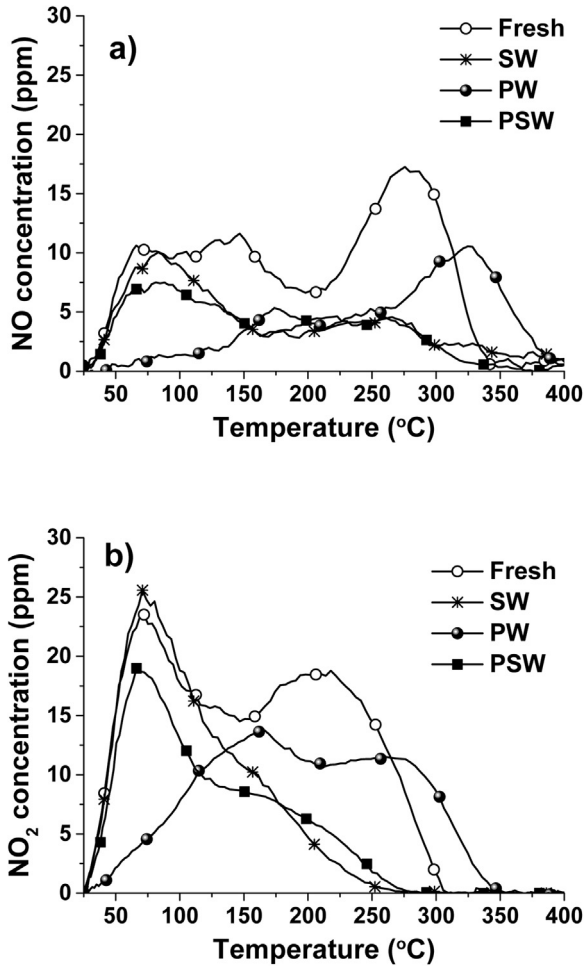

Fig. 5. NO (a) and NO_2 (b) desorption over fresh and treated Pt/SiO_2-ZrO_2 catalysts. *Pretreatment*: N_2 flow (500 ml/min), t = 15 min, T = 300 °C. *NO adsorption*: 1%NO/N_2 flow (30 ml/min), t = 30 min, T = 25 °C. *TPD run*: N_2 flow (1000 ml/min), heating rate = 20 °C/min.

Table 5
NO and NO_2 desorption from the SiO_2-ZrO_2 support and the Pt/SiO_2-ZrO_2 catalyst in NO-TPD.

Treatment	NO desorption [μmol/g]	NO_2 desorption [μmol/g]
Support		
Fresh	52	72
S	16 (−69%)	55 (−23%)
W	25 (−53%)	66 (−8%)
SW	22 (−59%)	52 (−27%)
PW	31 (−42%)	49 (−31%)
PSW	19 (−63%)	33 (−54%)
Catalyst		
Fresh	44	60
S	24 (−46%)	32 (−43%)
W	23 (−47%)	39 (−35%)
SW	23 (−48%)	40 (−33%)
PW	21 (−53%)	36 (−40%)
PSW	19 (−57%)	31 (−48%)

3.2. Effect of sulphur

The laboratory-scale accelerated sulphur treatment has been found to be an effective method to investigate the effect of sulphur on the catalyst [8,10,17,33,35]. In the study by Kärkkäinen et al. [10], XPS results revealed that the amount of S was 4.1 wt-% on the sulphur-treated Pt/Al_2O_3 catalyst. In comparison, the amount of sulphur adsorbed on the Pt/SiO_2-ZrO_2 catalyst was found to be

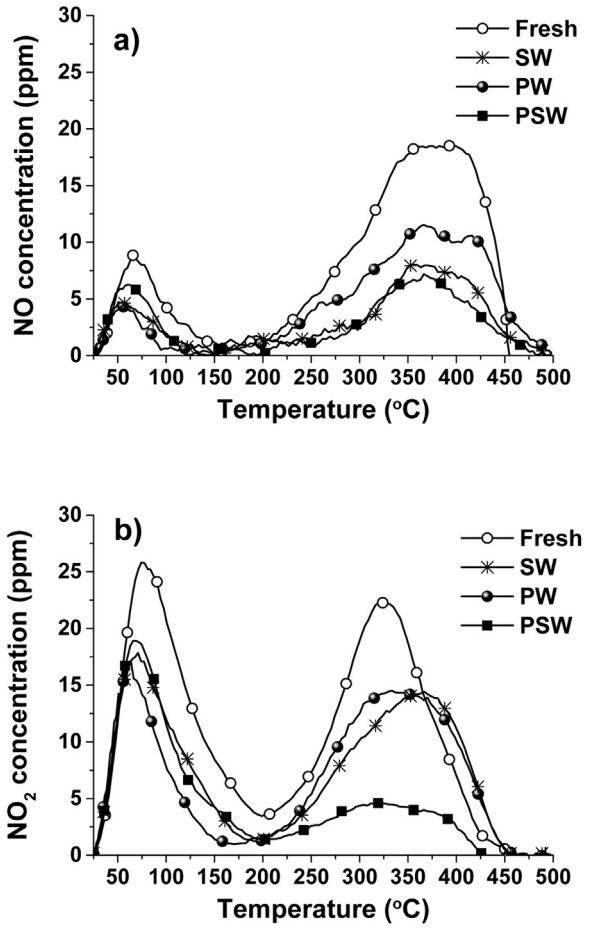

Fig. 6. NO (a) and NO_2 desorption over fresh and treated SiO_2-ZrO_2 supports. *Pre-treatment*: N_2 flow (500 ml/min), t = 15 min, T = 300 °C. *NO adsorption*: 1%NO/N_2 flow (30 ml/min), t = 30 min, T = 25 °C. *TPD run*: N_2 flow (1000 ml/min), heating rate = 20 °C/min.

lower in this study. The sulphur concentrations were below 1 wt-% on the S- and SW-treated Pt/SiO_2-ZrO_2 catalyst and SiO_2-ZrO_2 support according to the XPS results (Table 2). As the sulphur treatments were done similarly as our previous studies [e.g. 10], it can be concluded that the SiO_2-ZrO_2 support is more resistant to sulphur than the Al_2O_3 support. In Fig. 7a, the XPS spectra of sulphur in the inlet section of all measured samples are presented. The observed binding energies of the S 2p line indicate that sulphur is adsorbed as sulphate (SO_4^{2-}) on the S- and SW-treated samples (Table 1) [36].

According to the DRIFT results, no sulphur species were found on the S- and SW-treated Pt/SiO_2-ZrO_2 catalyst or SiO_2-ZrO_2 support (Fig. 1) due to the relatively low sulphur concentration. However, Park et al. [9] have observed in XRD studies that the formation of zirconium sulphate on Pt/SiO_2-ZrO_2 is still possible after 2 hours' SO_2-treatment at 400 °C in the presence of water [9].

The effect of the SW-treatment on the structure of the Pt/SiO_2-ZrO_2 catalyst and SiO_2-ZrO_2 support was studied by FESEM, TEM and XRD. According to the FESEM-EDS and TEM-EDS results, the amount of sulphur was very low (<1 wt-%) through the catalyst and support. These results are in good agreement with the XPS results. The morphological changes on the catalyst or support were negligible due to the SW-treatments. However, the average crystallite size of Pt was detected to increase slightly from 14 to 16 nm according to the XRD results (Table 3). A small increase in the crystallite size may indicate the presence of a reaction of SO_2 with oxygen at the Pt-O-support interface weakening the Pt–O interaction [37]. In addition, BET and BJH results indicate that the effect of sulphur on surface areas, pore volumes and pore sizes was minor (Table 6). In comparison with the fresh catalyst it can be seen that the S- and SW-treatments decreased the S_{BET} values, by 11 and 10%, respectively. The effect of these treatments on the BJH pore volumes and pore sizes was negligible. In the case of the SiO_2-ZrO_2 support, sulphur had also a negligible effect on the BET and BJH values.

Based on the activity test results, the S- and SW-treated Pt/SiO_2-ZrO_2 catalysts performed the same way as the fresh catalyst. From Fig. 8 and Table 4, it can be observed that sulphur (after the S- and SW-treatments) had a negligible effect on the CO and C_3H_6 conversions as well as the N_2O formation. Furthermore, the S-treatment had no effect on the NO conversion but the addition of 10 vol-% of water with sulphur (SW-) caused the NO conversion to decrease by ca. 10% at temperatures above 240 °C. According to the NO-TPD results, the SW-treatment had only a minor effect on the NO and NO_2 desorption at low temperatures (<100 °C) over the Pt/SiO_2-ZrO_2 catalyst (Figs. 5 and 6). Alternatively, the SW-treatment decreased the amounts of strongly adsorbed NO and NO_2 at higher temperatures (>200 °C). The loss of these strongly adsorbed NO_x species is probably due to the reaction between the basic hydroxyl groups of ZrO_2 and sulphates, which has proven to prevent the formation of stable nitrates [38]. The total amount of desorbed NO and NO_2 decreased after the SW-treatments (Table 5) which is possibly limiting the NO conversion. Similarly, to the Pt/SiO_2-ZrO_2 catalyst, the S- and SW-treatments were proven to decrease the NO and NO_2 desorption over the SiO_2-ZrO_2 support.

The activity of the Pt/SiO_2-ZrO_2 catalyst was still high after the sulphur treatments. The high resistance towards SO_2 could be due to our support material. According to Kim et al. [12], the

Table 6
The BET surface areas, BJH pore volumes and BJH pore sizes of the SiO_2-ZrO_2 support and the Pt/SiO_2-ZrO_2 catalyst. The difference between fresh and treated samples is presented in brackets.

	BET surface area [m^2/g]	BJH pore volume [cm^3/g]	BJH pore size [nm]
Support			
Fresh	113	0.20	7.0
S	113 (±0%)	0.20 (+2%)	7.1 (+2%)
W	113 (±0%)	0.20 (+2%)	7.1 (+2%)
SW	108 (−4%)	0.19 (−2%)	7.1 (+2%)
PW	50 (−56%)	0.11 (−45%)	8.7 (+25%)
PSW	60 (−47%)	0.13 (−37%)	8.4 (+20%)
Catalyst			
Fresh[a]	119	0.22	7.8
S	106 (−11%)	0.22 (−2%)	7.2 (−8%)
W	112 (−7%)	0.21 (−4%)	8.0 (+3%)
SW[a]	108 (−10%)	0.21 (−6%)	8.1 (+4%)
PW[a]	72 (−39%)	0.17 (−22%)	8.6 (+10%)
PSW[a]	31 (−74%)	0.11 (−51%)	13.4 (+73%)

[a] Adapted from Ref. [17].

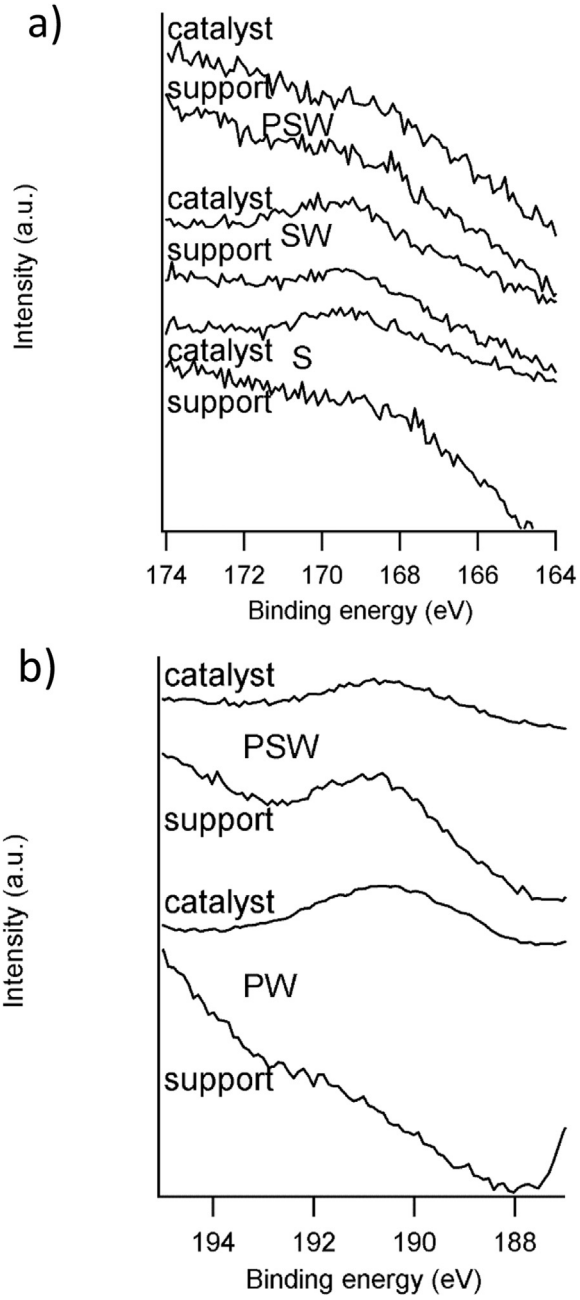

Fig. 7. S 2p (a) and P 2s (b) photoelectron lines measured with XPS at the inlet sections of the catalyst and the support after different treatments.

ZrO_2 compound enhances interaction between Pt and the support that improves catalyst stability towards sulphur poisoning. In addition, SiO_2 has a low basicity that can prevent SO_2 poisoning [12]. A good resistance towards SO_2 can also be observed from the relatively low amount of adsorbed sulphur, shown by XPS, FESEM-EDS and TEM-EDS. In addition, sulphur had no significant effect on the Pt/SiO_2-ZrO_2 catalyst's structure, based on the results of SEM, TEM, BET and BJH. Thus, it can be concluded that the Pt/SiO_2-ZrO_2 catalyst has a good resistance towards SO_2 in comparison with the widely used Pt/Al_2O_3 catalyst shown by our previous studies and the literature [8–10]. In the case of the Pt/Al_2O_3 catalyst, sulphur compounds were proven to decrease the specific surface area and further on the catalyst activity in C_3H_6 and CO oxidations [8,10]. However, these effects on the Pt/SiO_2-ZrO_2 catalyst were not detected.

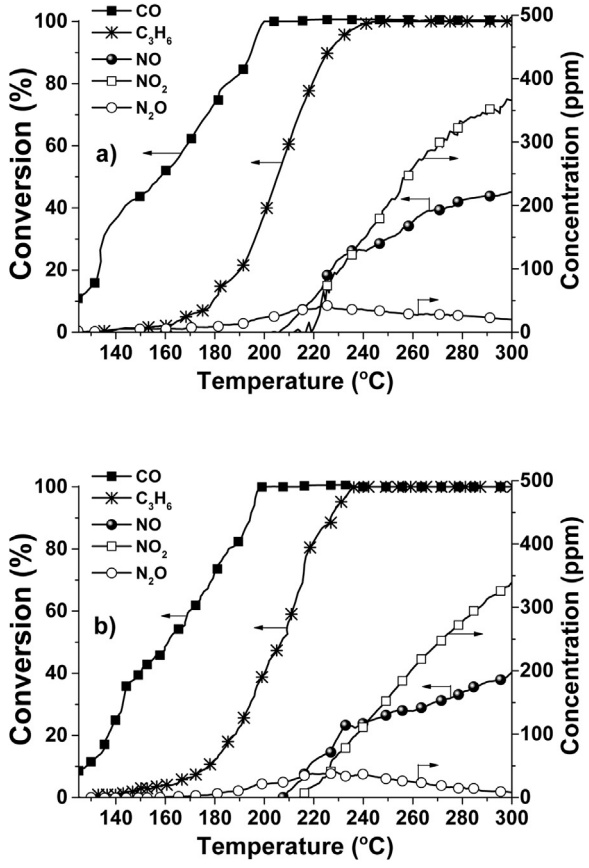

Fig. 8. CO, C_3H_6 and NO conversions (black symbols) as well as NO_2 and N_2O formation (white symbols) over S- (a) and SW-treated (b) Pt/SiO_2-ZrO_2 catalyst as a function of temperature. Reaction gas mixture: 500 ppm CO, 300 ppm C_3H_6, 1000 ppm NO, 10 vol-% H_2O, 12 vol-% O_2 and balance N_2. Heating rate: 5 °C/min, Total flow: 1000 ml/min, GHSV: 34,000 h^{-1}.

3.3. *Effect of phosphorus*

Our earlier studies [31,39] have shown that the accelerated phosphorus (PW) treatment is a suitable method to study the effect of phosphorus on the catalyst. The XPS results have revealed that the amount of P was 7–9 wt-% on the Pt/Al_2O_3 and the $PtPd/Al_2O_3$ diesel oxidation catalysts after the PW-treatment [31]. According the XPS results of this study, the phosphorus concentration on the PW-treated Pt/SiO_2-ZrO_2 catalyst was 7–8 wt-% (Table 2). In addition, the P concentration on the catalyst was consistently higher in the inlet than in the outlet of the monolithic catalyst. The binding energy values of the P 2s line suggest that phosphorus is adsorbed as phosphate (PO_4^{3-}) on the catalyst surface (Fig. 7b) [18]. Phosphorus species were also detected from the DRIFT results. The PW-treatments shifted the broad band maxima from 1140 to 1300 cm^{-1} to higher wavenumbers which could be assigned as the asymmetric stretching vibrations of phosphate (Fig. 1) [40,41]. In addition, the XPS studies revealed that the PW-treatments had no effect on the oxidation state of Pt on the catalyst as only metallic Pt was detected before and after the treatments.

The adsorption of phosphorus and surface structure changes during the PW-treatment on the Pt/SiO_2-ZrO_2 catalyst and SiO_2-ZrO_2 support were studied by FESEM, TEM and XRD. The cross-sectional FESEM samples were prepared from the inlet and outlet parts of the catalyst and support. According to the FESEM-EDS point and line analyses from the cross-sectional samples, around 5 wt-% of phosphorus was detected throughout the Pt/SiO_2-ZrO_2 and SiO_2-ZrO_2 catalyst samples. However, a quantitative

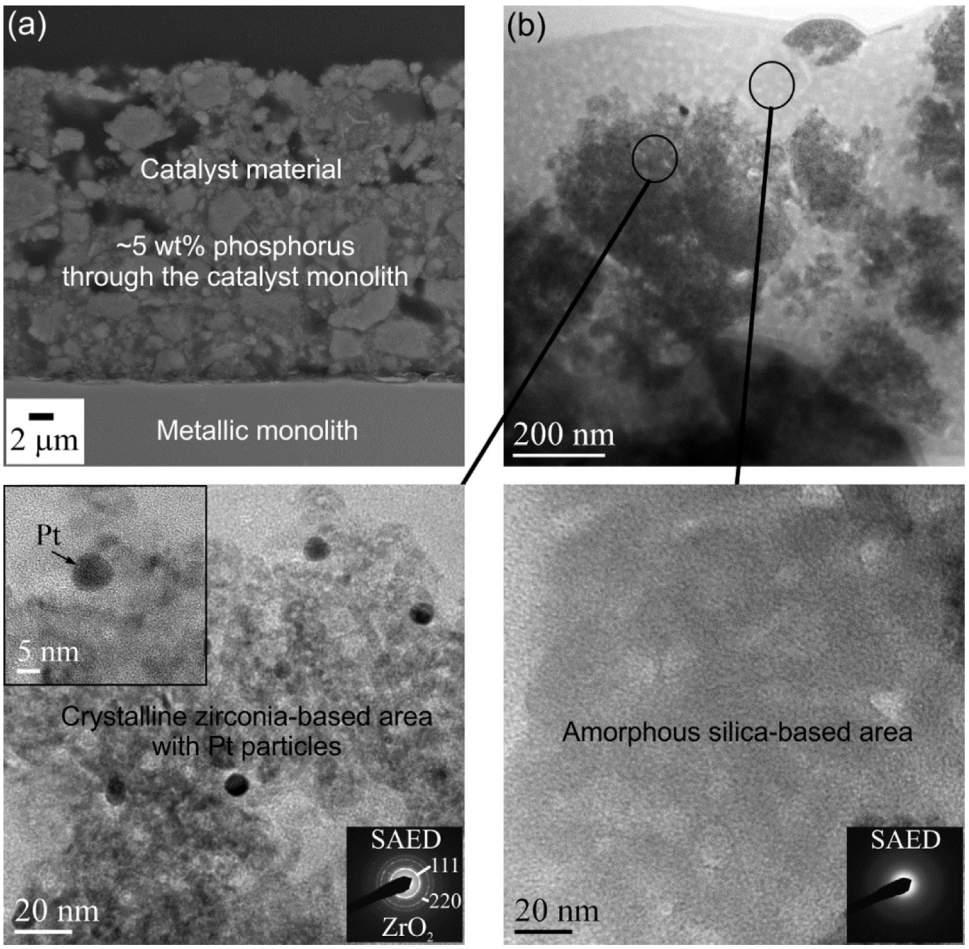

Fig. 9. The PW-treated Pt/SiO_2-ZrO_2 catalyst, (a) the cross-sectional FESEM image and (b) the cross-sectional TEM images, higher magnification images with SAED patterns from the corresponding areas.

analysis of the exact amount of phosphorus on the catalyst by EDS is challenging due to the overlapping of the P Kα, Zr Lα, and Pt Mα peaks. No significant morphological changes were detected with TEM in the PW-treated Pt/SiO_2-ZrO_2 catalyst (Fig. 9) or SiO_2-ZrO_2 support compared to the fresh ones. Instead, the aluminium oxide (Al_2O_3-) based catalysts have revealed that phosphorus accumulates on the surface of the Al_2O_3 based catalysts and changes the catalyst structure from a crystalline to an amorphous form [31,42]. Thus, based on the results gained the SiO_2-ZrO_2 based catalysts have a much better resistance towards phosphorus poisoning than the Al_2O_3 based catalysts. Nevertheless, the XRD results revealed that the PW-treatment increases slightly the average crystallite size of Pt (from 14 to 18 nm) (Table 3) similarly to studies with the Al_2O_3 based catalysts [42,43]. In addition, the BET and BJH results (Table 6) indicate that phosphorus affects the porous structure of the Pt/SiO_2-ZrO_2 catalyst as the PW-treatments decrease the specific surface areas and pore volumes of the Pt/SiO_2-ZrO_2 catalyst by 39 and 22%, respectively. In the case of the parent SiO_2-ZrO_2 support, phosphorus decreased the surface areas and pore volumes by 56 and 45%, respectively.

In the activity tests, the effect of phosphorus was that the CO and C_3H_6 light-off temperatures (T_{90}) increased by 30 °C and 45 °C, respectively (Table 4). Phosphorus (PW-treatment) decreased the CO and C_3H_6 conversions over the Pt/SiO_2-ZrO_2 catalyst over the entire tested temperature range (Fig. 10a). In addition, the activity test results prove that phosphorus had a significant impact on the NO conversion over the Pt/SiO_2-ZrO_2 catalyst since the conversion decreased by 20 percentage points at temperatures above 230 °C. Similarly, the PW-treatments decreased the amount of desorbed NO and NO_2 species in the NO-TPD studies especially at low temperatures (Fig. 5, Table 5). Thus, the loss of the active sites for NO_x adsorption might be limiting the NO oxidation to NO_2 over the PW-treated catalyst in the activity tests. Similarly to our previous studies [6,31], phosphorus also decreases the catalyst activities and specific catalyst surface areas of the studied materials. The activity loss is probably due to the formation of phosphates blocking the accessibility of reacting molecules to the active sites. The results gained are in good agreement e.g. with the results by Hauff et al. [44] which highlight that the activity of DOCs have proven to be dependent on the catalyst surface area.

3.4. The co-effect of phosphorus and sulphur

The co-exposure of phosphorus and sulphur (PSW) on the Pt/SiO_2-ZrO_2 catalyst and the SiO_2-ZrO_2 support were also studied. In the case of the PSW-treated catalyst, the presence of phosphorus clearly dominated over that of sulphur. In general, the XPS results for the PSW-treated sample were similar to those of the PW-treated sample, although the phosphorus concentration was 4–5% higher in the latter one (Table 2). In addition, the amount of phosphorus was around two percentage points lower on the SiO_2-ZrO_2 support compared to the Pt/SiO_2-ZrO_2 catalyst. Similarly, to the PW-treated samples, the binding energies of the PSW-treated samples indicate that phosphorus is adsorbed as PO_4^{3-} (Fig. 7b, Table 1). Alternatively, sulphur was not detected in the inlet of the PSW-treated monolithic samples (Fig. 7a). However, a minor S 2p line

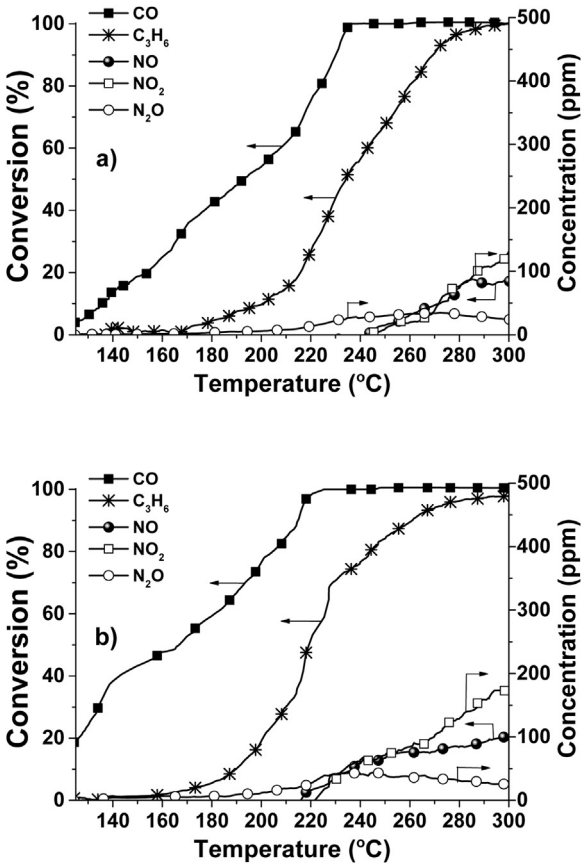

Fig. 10. CO, C_3H_6 and NO conversions (black symbols) as well as NO_2 and N_2O formation (white symbols) over PW- (a), and PSW-treated (b) Pt/SiO_2-ZrO_2 catalysts as a function of temperature. Reaction gas mixture: 500 ppm CO, 300 ppm C_3H_6, 1000 ppm NO, 10 vol-% H_2O, 12 vol-% O_2 and balance N_2. Heating rate: 5 °C/min, Total flow: 1000 ml/min, GHSV: 34,000 h^{-1}.

was observed in the outlet part of the monolith indicating sulphur being adsorbed most probably in the form of SO_4^{2-}. Because sulphur was found only in the outlet part of the PSW-treated monolith sample it can be concluded that phosphorus has a role in preventing sulphur adsorption on the Pt/SiO_2-ZrO_2 catalysts. In accordance with the XPS results, sulphur compounds were not detected on the PSW-treated catalyst surface by DRIFT. Furthermore, the shift of the broad band maximum (1248 cm^{-1}) to higher wavenumbers (1267 cm^{-1}) indicates the presence of phosphate species on the PSW-treated catalysts (Fig. 1).

The effects of the PSW-treatment on the structure and performance of the Pt/SiO_2-ZrO_2 catalyst and the SiO_2-ZrO_2 support were studied by FESEM, TEM, XRD and activity tests. The cross-sectional FESEM samples were prepared from the inlet and outlet parts of the catalyst and support. The phosphorus concentration on the PSW-treated samples is close to the P concentration measured after the PW-treatment. Based on the FESEM-EDS point and line analyses from the cross-sectional samples, ~5 wt-% phosphorus was detected through the PSW-treated samples. The phosphorus concentration is probably higher in the sample inlet than outlet but an exact quantitative analysis of phosphorus cannot be done due to the overlapping peaks in the EDS analyses. The amount of sulphur determined by EDS was low (<1 wt-%) through the Pt/SiO_2-ZrO_2 catalyst and the SiO_2-ZrO_2 support, which is in good agreement with the XPS results. No significant morphological changes were detected with TEM in the PSW-treated samples compared to the fresh ones. However, the XRD results revealed that the PSW-treatment may increase the average crystallite size of Pt in the catalyst from 14 nm to 16 nm (Table 3). The morphological changes were also observed from the BET and BJH results that indicate the decrease in the specific surface area and pore volumes of the studied samples due to the PSW-treatment (Table 6).

The co-exposure of sulphur and phosphorus (PSW-treatment) decreased the activity of the Pt/SiO_2-ZrO_2 catalyst in the oxidation of C_3H_6 and CO (Fig. 10b). The activity loss is probably due to the decrease in the BET surface area and pore volumes (Table 6). However, the CO and C_3H_6 light-off temperatures (T_{50} and T_{90}) over the PSW-treated catalyst were 9–15 °C lower than in the case of the PW-treated catalyst (Table 4). In addition, the amount of phosphorus was also proven to be lower on the PSW-treated Pt/SiO_2-ZrO_2 catalyst compared to the PW-treated catalyst. Thus, the reason for differences in the catalyst behaviour after the treatments could be due to that phosphorus is competing the adsorption sites with sulphur and the interactions between these impurities and catalyst surface are possible. However, the explanation of simultaneous adsorption of P and S on the SiO_2-ZrO_2 based catalysts will require further studies. Furthermore, the NO conversion maximum (21%) was higher in the case of the PSW-treated catalyst compared to the PW-treated catalyst (17%). The reason could be that the PSW-treated catalyst has a higher amount of weakly adsorbed NO_x species shown by NO-TPD (Fig. 5). These weakly adsorbed NO_x species could be the most active species in the NO oxidation to NO_2.

4. Conclusions

In this study, the effect of water, sulphur and phosphorus treatments on a Pt/SiO_2-ZrO_2 diesel oxidation catalyst was investigated. Thus, the S-, W-, SW-, PW- and PSW-treatments on the Pt/SiO_2-ZrO_2 catalyst were done. The fresh and treated Pt/SiO_2-ZrO_2 catalysts were characterized and their activity was studied in lean diesel exhaust conditions. Sulphur and water treatments had a negligible effect on the activity of the Pt/SiO_2-ZrO_2 catalyst. Although a low amount of sulphur was found on catalysts, the activity remained high probably due to the good resistance of the SiO_2-ZrO_2 support towards SO_2. Alternatively, phosphorus concentration was high throughout the treated Pt/SiO_2-ZrO_2 catalyst and SiO_2-ZrO_2 support shown by the XPS and FESEM-EDS results. Phosphorus also affected the catalyst performance due to a decrease in the CO, NO and C_3H_6 conversions. The reason for the lower activity is possibly the formation of phosphates that are decreasing the specific surface area of a catalyst. Thus, the access of the reactants to the catalyst pores and active sites is hindered. Both sulphur and phosphorus also increased the crystallite size of Pt in the treated Pt/SiO_2-ZrO_2 catalysts. However, sulphur inhibited the poisoning effect of phosphorus. After the co-exposure to P and S, the catalyst activity was higher and the amount of phosphorus was lower compared to the phosphorus treated catalyst.

Based on the results, phosphorus compounds cause slight morphological changes in Pt/SiO_2-ZrO_2 and decrease its catalytic performance. However, Pt/SiO_2-ZrO_2 is found to be more resistant towards phosphorus poisoning than the Al_2O_3-based catalysts. Alternatively, Pt/SiO_2-ZrO_2 was proven to be a promising catalyst for applications that use fuels which contain sulphur. Thus, it is possible to install the Pt/SiO_2-ZrO_2 catalyst containing DOC unit close to the diesel engine also in stationary and marine applications where sulphur removal units, e.g. scrubbers, might be required. In addition, sulphur-resistant catalyst materials are needed especially in emerging markets where catalysts might be exposed to high sulphur fuel exhaust gases. Thus, this study provides valuable information that can be utilized in designing sulphur-tolerant DOC systems for diesel vehicles.

Acknowledgement

The authors acknowledge the Academy of Finland (ACABIO project, 139187) for the financial support.

References

[1] Directive 715/2007/EC of the European Parliament and Council.
[2] C.T. Bowman, in: W. Bartok, A.F. Sarofim (Eds.), Fossil Fuel Combustion, John Wiley & Sons Inc, New York, 1991, pp. 215–260.
[3] S.J. Smith, J. van Aardenne, Z. Klimont, R.J. Andres, A. Volke, S. Delgado Arias, Atmos. Chem. Phys. 11 (2011) 1101–1116.
[4] J. Andersson, M. Antonsson, L. Eurenius, E. Olsson, M. Skoglundh, Appl. Catal. B: Environ. 72 (2007) 71–81.
[5] A. Winkler, P. Dimopoulos, R. Hauert, C. Bach, M. Aguirre, Appl. Catal. B: Environ. 84 (2008) 162–169.
[6] V. Kröger, M. Hietikko, D. Angove, D. French, U. Lassi, A. Suopanki, R. Laitinen, R.L. Keiski, Top. Catal. 42–43 (2007) 409–413.
[7] O. Kröcher, M. Widmer, M. Elsener, D. Rothe, Ind. Eng. Chem. Res. 48 (2009) 9847–9857.
[8] T. Kolli, T. Kanerva, M. Huuhtanen, M. Vippola, K. Kallinen, T. Kinnunen, T. Lepistö, J. Lahtinen, R.L. Keiski, Catal. Today 154 (2010) 303–307.
[9] S.M. Park, H.-G. Jang, E.S. Kim, H.-S. Han, G. Seo, Appl. Catal. A: Gen. 427–428 (2012) 155–164.
[10] M. Kärkkäinen, M. Honkanen, V. Viitanen, T. Kolli, A. Valtanen, M. Huuhtanen, K. Kallinen, M. Vippola, T. Lepistö, J. Lahtinen, R.L. Keiski, Top. Catal. 56 (2013) 672–678.
[11] D. Chan, S. Tischer, J. Heck, C. Diehm, O. Deutschmann, Appl. Catal. B: Environ. 156–157 (2014) 153–165.
[12] M.-Y. Kim, J.-S. Choi, T.J. Toops, E.-S. Jeong, S.-W. Han, V. Schwartz, J. Chen, Catalysts 3 (2013) 88–103.
[13] M. Lakshmi Kantam, B. Purna Chandra Rao, R. Sudarshan Reddy, N.S. Sekhar, B. Sreedhar, B.M. Choudary, J. Mol. Catal. A: Chem. 272 (2007) 1–5.
[14] Y. Wang, R. Wu, Y. Zhao, Catal. Today 158 (2010) 470–474.
[15] J. Dawody, M. Skoglundh, L. Olsson, E. Fridell, J. Catal. 234 (2005) 206–218.
[16] J.K. Lampert, M.S. Kazi, R.J. Farrauto, Appl. Catal. B: Environ. 14 (1997) 211–223.
[17] A. Väliheikki, T. Kolli, M. Honkanen, O. Heikkinen, M. Kärkkäinen, K. Kallinen, M. Huuhtanen, M. Vippola, J. Lahtinen, R.L. Keiski, Top. Catal. 60 (2017) 307–311.
[18] A.V. Naumkin, A. Kraut-Vass, S.W. Gaarenstroom, C.J. Powell, NIST (National Institute of Standards and Technology) X-ray Photoelectron Spectroscopy Database. http://srdata.nist.gov/xps/Default.aspx (Accessed 10.01.15).
[19] M.S. Wong, H.C. Huang, J.Y. Ying, Chem. Mater. 14 (2002) 1961–1973.
[20] G. Fan, M. Shen, Z. Zhang, F. Jia, J. Rare Earth 27 (2009) 437–442.
[21] H. Chen, C. Deng, X. Zhang, Angew. Chem. Int. Ed. 49 (2010) 607–611.
[22] M. Andrianainarivelo, R. Corriu, D. Leclercq, P.H. Mutin, A. Vioux, J. Mater. Chem. 6 (1996) 1665–1671.
[23] W. Fang, X. Chen, N. Zheng, J. Mater. Chem. 20 (2010) 8624–8630.
[24] H. Launay, S. Loridant, A. Pigamo, J.L. Dubois, J.M.M. Millet, J. Catal. 246 (2007) 390–398.
[25] T. Otsuka, Y. Chujo, Polym. J. 42 (2010) 58–65.
[26] M. Wang, Z. Si, L. Chen, X. Wu, J. Yu, J. Rare Earth 31 (2013) 1148–1156.
[27] K. Rahkamaa-Tolonen, T. Maunula, M. Lomma, M. Huuhtanen, R.L. Keiski, Catal. Today 100 (2005) 217–222.
[28] M. Devadas, O. Kröcher, M. Elsener, A. Wokaun, N. Söger, M. Pfeifer, Y. Demel, L. Mussmann, Appl Catal. B: Environ. 67 (2006) 187–196.
[29] O. Kröcher, M. Widmer, M. Elsener, D. Rothe, Ind. Eng. Chem. Res. 48 (2009) 9847–9857.
[30] M. Khosravi, C. Sola, A. Abedi, R.E. Hayes, W.S. Epling, M. Votsmeier, Appl. Catal. B: Environ. 147 (2014) 264–274.
[31] M. Kärkkäinen, T. Kolli, M. Honkanen, O. Heikkinen, M. Huuhtanen, K. Kallinen, T. Lepistö, J. Lahtinen, M. Vippola, R.L. Keiski, Top. Catal. 58 (2015) 961–970.
[32] A. Väliheikki, T. Kolli, M. Huuhtanen, T. Maunula, T. Kinnunen, R.L. Keiski, Conference paper in east meets west on innovation and entrepreneurship, Conference Proceedings (2012) 327–334 (ISBN: 978-9963-700-57-8).
[33] A. Väliheikki, T. Kolli, M. Huuhtanen, T. Maunula, R.L. Keiski, Top. Catal. 58 (2015) 1002–1011.
[34] J. Zuo, Z. Chen, F. Wang, Y. Yu, L. Wang, X. Li, Ind. Eng. Chem. Res. 53 (2014) 2647–2655.
[35] M. Honkanen, M. Kärkkäinen, T. Kolli, O. Heikkinen, V. Viitanen, L. Zeng, H. Jiang, K. Kallinen, M. Huuhtanen, R.L. Keiski, J. Lahtinen, E. Olsson, M. Vippola, Appl. Catal. B: Environ. 182 (2016) 439–448.
[36] J.F. Moulder, Handbook of X-ray Photoelectron Spectroscopy: a Reference Book of Standard Spectra for Identification and Interpretation of XPS Data, Perkin Elmer, Eden Prairie, 1992.
[37] A.F. Lee, K. Wilson, R.M. Lambert, C.P. Hubbard, R.G. Hurley, R.W. McCabe, H.S. Gandhi, J. Catal. 184 (1999) 491–498.
[38] H.Y. Law, J. Blanchard, X. Carrier, C. Thomas, J. Phys. Chem. C 114 (2010) 9731–9738.
[39] V. Kröger, U. Lassi, K. Kynkäänniemi, A. Suopanki, R.L. Keiski, Chem. Eng. J. 120 (2006) 113–118.
[40] M. Mami, H. Oudadesse, R. Dorbez-Sridi, H. Capiaux, P. Pellen-Mussi, D. Chauvel-Lebret, H. Chaair, G. Cathelineau, Ceram. -Silik. 52 (2008) 121–129.
[41] Y.-K. Lee, K.-N. Kim, S.-Y. Choi, J. Biomed. Mater. Res. 49 (2000) 233–237.
[42] M. Honkanen, M. Kärkkäinen, O. Heikkinen, K. Kallinen, T. Kolli, M. Huuhtanen, J. Lahtinen, R.L. Keiski, T. Lepistö, M. Vippola, Top. Catal. 58 (2015) 971–996.
[43] S.K. Matam, E.V. Kondratenko, M.H. Aguirre, P. Hug, D. Rentsch, A. Winkler, A. Weidenkaff, D. Ferri, Appl. Catal. B: Environ. 129 (2013) 214–224.
[44] K. Hauff, U. Tuttlies, G. Eigenberger, U. Nieken, Appl. Catal. B: Environ. 100 (2010) 10–18.